



#### **ENVIRONMENTAL SCIENCE**

ISSN 0250-3301 CODEN HCKHDV **HUANJING KEXUE** 

城市污水再生处理中微量有机污染物控制的关键难题与解决思路 王文龙,吴乾元,杜烨,黄南,陆韻,魏东斌,胡洪营







2021年6月

第42卷 第6期 Vol.42 No.6

## 採货箱 (HUANJING KEXUE)

#### ENVIRONMENTAL SCIENCE

第42卷 第6期 2021年6月15日

#### 目 次

综述与专论	
城市环境生物安全研究的进展与挑战	2565)
城市污水再生处理中微量有机污染物控制的关键难题与解决思路 王文龙、吴乾元、杜烨、黄南、陆韻、魏东斌、胡洪莹(2	2573)
污泥 EPS 作为阻燃剂的机制归纳与潜力分析	2583)
研究报告	.505)
	1505 )
北京大气 PM <sub>2.5</sub> 载带金属浓度、来源及健康风险的城郊差异 ············ 周安琪,刘建伟,周旭,毕思琪,张博晗,高越,曹红斌(2京津冀及周边 MAIAC AOD 和 PM <sub>2.5</sub> 质量浓度特征及相关性分析 ······················· 金团因,杨兴川,晏星,赵文吉(2	.393 )
示律異及同边 MAIAU AUD 和 PM <sub>2.5</sub> 贝里 体 及 付 征 及 相 大 性 方 竹	.004 )
天津市 PM <sub>2.5</sub> 中二次硝酸盐形成及防控 肖致美, 武婷, 卫昱婷, 徐虹, 李立伟, 李鹏, 陈魁, 邓小文 (2	.616)
南京市大气细颗粒物(PM <sub>2.5</sub> )中硝基多环芳烃污染特征与风险评估 傅银银,文浩哲,王向华,于南洋,李冰,韦斯(2	(626)
汾渭平原吸收性气溶胶时空演化及潜在源区分析 刘旻霞,李亮,于瑞新,宋佳颖,张国娟,穆若兰,徐璐(2	:634)
西南典型区域夏李大气含氧挥发性有机化合物来源解析	
… 陈木兰,王赛男,陈天舒,朱波,彭超,周佳维,车汉雄,黄汝辉,杨复沫,刘合凡,潭钦文,韩丽,陈军辉,陆克定,陈阳(2	2648)
气溶胶中溶解性有机质(DOM)液相氧化 ····································	2659)
某于 MERRA-2 再分析资料的上海市近 40 年大与里碳浓度变化及潜在来源解析	
曹闪闪,段玉森,高婵婵,苏玲,杨怡萱,张洋,蔡超琳,刘敏(2 石家庄市臭氧和二氧化氮的时空演替特征及来源解析	2668)
石家庄市皇菊和一菊化菊的时空演替特征及来源解析	2679)
其工来化學投稿注的邯郸市自氨化成铂值版性	2601 )
全 J Landsat 双加印入干面地版地 AOD 叫工作用及观中化的关键。	.077 ) 1712 )
基丁上生	./13 )
中原项印件国家下线公路 SUA 生成省野市异	./21 )
北京中"大气十余"实施的全气质量以香效益	7/30)
上业大气污染源排放绩效定量评价及应用	.740)
基于生态风险的我国水环境高风险抗生素筛选排序	:748)
基于 Landsat 数据的天甲盆地腹地 AOD 的 全	2758)
基于模型研究质量评价的 SWAT 模型参数取值特征分析	2769)
大型浅水湖泊水质模型边界负荷敏感性分析 王亚宁, 李一平, 程月, 唐春燕, 陈刚 (2	2778)
不同流域水陆过渡带氮磷有效态的特征对比及环境意义 朱海,袁旭音,叶宏萌,成瑾,毛志强,韩年,周慧华(2	2787)
基于不同赋权方法的北运河上游潜在非点源污染风险时空变化特征分析	,
李华林,张建军,张耀方,常国梁,时迪迪,徐文静,宋卓远,于佩丹,张守红(2	2796)
长期施肥和耕作下紫色土坡耕地经流 TN 和 TP 流生特征	2810)
长期施肥和耕作下紫色土坡耕地径流 TN 和 TP 流失特征 ····································	2817)
太湖流域上游南苕溪水系夏秋季水体溶存二氧化碳和甲烷浓度特征及影响因素	.017)
源件器 田州州 用油目 化治园 化大大 何又言 茹茹江 (2	1926)
保置牌、口垛垛、周开立、水海网、水万万、阳至岩、紫灰江(2 低温期浅水湖泊氮的分布及无机氮扩散通量:以白洋淀为例 文艳,单保庆、张文强(2 覆盖条件下底泥微环境对内源磷释放的影响 陈姝彤,李大鹏,徐楚天,张帅,丁玉琴,孙培荣,黄勇(2 圩区河道底泥腐殖酸对重金属和抗生素的共吸附 薛向东,杨宸豪,于荐麟,庄海峰,方程冉(2 两种 PPCPs 对雅鲁藏布江沉积物硝化作用的影响 凌欣,徐慧平,陆光华(2	1020 )
版 通知仅外面问题的另中区人们就让 取进里:以口什使为例 大把, 字下页, 取入速 (2) 大型, 字下页, 取入速 (2) 大型, 字下面, 如人地, 立上题, 丛林工, 卫地, 工工程, 刀齿龙, 生量 (2)	.039 )
復 面余件下版池 國外現別 内原瞬释 放的影响	2848 )
<b>叶区河</b> 垣底泥腐殖散对里金属和机生系的共败附	.856 )
两种 PPCPs 对雅鲁藏布江沉枳物硝化作用的影响	(868)
铁碳微电解及沸石组合人工湿地的废水处理效果 ····································	1875)
CDs-BOC 复合催化剂可见光下活化过硫酸盐降解典型 PPCPs 雷倩, 许路, 艾伟, 李志敏, 杨磊 ( 2	2885)
pg-C <sub>3</sub> N <sub>4</sub> /BiOBr/Ag 复合材料的制备及其光催化降解磺胺甲哌唑 ······· 杨利伟,刘丽君,夏训峰,朱建超,高生旺,王洪良,王书平(2	2896)
海藻酸钠负载硫化零价铁对水体中 $Cr(VI)$ 的还原去除·················王旭,杨欣楠,黄币娟,刘壮,牟诗萌,程敏,谢燕华(2 超顺磁性纳米 $Fe_3O_4$ @ $SiO_2$ 功能化材料对镉的吸附机制····································	2908)
超顺磁性纳米 Fe, O, @ SiO, 功能化材料对镉的吸附机制 张立志, 易平, 方丹丹, 王强(2	2917)
典型药物在医院废水和城市污水处理厂中的污染特征及去除情况 叶璞,游文丹,杨滨,陈阳,汪立高,赵建亮,应光国(2	2928)
印染废水循环利用抗牛素抗性基因丰度变化特性	2937)
短程硝化反硝化除磷颗粒污泥的同步驯化····································	946)
医葡萄萄化颗粒污泥的长期保藏及快速活性恢复	957)
市政运泥执敏计程由市全属迁移特性及环境效应证估。	2966)
不同体物农口上榷拾小麦并州其田夕祥州	2075 )
不同作物农田土壤抗生素抗性基因多样性····································	.973 ) 1001 \
温度和搅拌对牛粪厌氧消化系统抗生素抗性基因变化和微生物群落的影响	.901 )
温度和现任对于美质氧消化系统优生系优性基因变化和减生物群落的影响	1002
大孩子, 家伙伴, 木入游, 条押, 木又将, 庞小竹, 贬 ( )	.992)
小麦秸秆生物质炭施用对不同耕作措施土壤碳含量变化的影响	(000
农牧交错带典型区土壤氮磷空间分布特征及其影响因素 … 张燕江,王俊鹏,王瑜,张兴昌,甄庆,李鹏飞(3	010)
汞矿区周边土壤重金属空间分布特征、污染与生态风险评价 王锐, 邓海, 贾中民, 王佳彬, 余飞, 曾琴琴 (3	018)
调理剂对磷镉富集土壤中两种元素交互作用的影响 黄洋, 胡学玉, 曹坤坤, 张敏, 胡晓晓, 王子劲 (3	028)
S-烯丙基-L-半胱氨酸缓解水稻种子幼根和幼芽镉胁迫机制 ·········· 程六龙、黄永春、王常荣、刘仲齐、黄益宗、张长波、王晓丽(3	(037
连续4个生长季大气CO <sub>2</sub> 升高与土壤铅(Pb)污染耦合下刺槐幼苗根际土壤微生物特征 ····································	
では、	046)
嗜热脂肪地芽胞杆菌对聚苯乙烯的降解性能	3056)
冬青和女贞叶表面颗粒物微形态及叶际细菌群落结构 李慧娟 徐爱玲 乔凤禄 蔣敏 宋琪(3	3063
罗红霉素对大型潘牛殖生长及抗氧化系统的影响	3074
中国粮食作物产量和木本植物生物量与地表臭氧污染的响应关系	3084)
《环境科学》征订启事(2698) 《环境科学》征稿简则(2712) 信息(3027, 3055, 3073)	<i>,</i> ,
#. 1.1941-14 # PEN-1941-14 # PEN-194	



# CDs-BOC 复合催化剂可见光下活化过硫酸盐降解典型 PPCPs

雷倩, 许路, 艾伟, 李志敏, 杨磊\*

(西安建筑科技大学环境与市政工程学院, 西安 710055)

摘要:本研究通过简便的水热和煅烧两步法合成了一种新型光催化剂,该方法用碳量子点(CDs)修饰 BiOCl 纳米片. 制备的纳米复合材料(CDs-BOC)通过 X 射线衍射(XRD)、扫描电子显微镜(SEM)、高分辨率透射电子显微镜(HRTEM)、紫外-可见漫反射吸收光谱(DRS)、X 射线光电子能谱(XPS)和稳态荧光光谱(PL)等手段进行了表征. 结果表明,此材料成功地引入了CDs. 7% CDs-BOC 纳米复合材料的光吸收边界被增强至可见光区域(424 nm),并提高了光致电子-空穴对的分离效率. 为了提高有机污染物降解的效果,过硫酸盐(PS)被引入了 CDs-BOC 光催化体系中. 由于复合纳米催化剂具有出色的光催化能力,光生电子可以有效活化 PS,产生更多的活性氧化物质. 在可见光( $\lambda$  > 420 nm)照射下, 20 min 内可以完全去除 5 mg·L <sup>-1</sup>对-乙酰氨基酚(AAP). 通过自由基淬灭实验和电子顺磁共振波谱(EPR),探明了此体系具有多种活性氧化物质: ·OH、·SO<sub>4</sub> 、·O<sub>2</sub> 和 h \* ,并提出了降解反应机制. 以上结果体现出 CDs-BOC/PS 体系在光催化处理水污染方面具有广阔的应用前景.

关键词:可见光催化; 过硫酸盐活化; 碳量子点; 活性氧化物质; 对-乙酰氨基酚(AAP)

中图分类号: X703.1 文献标识码: A 文章编号: 0250-3301(2021)06-2885-11 DOI: 10.13227/j. hjkx. 202011047

# CDs-BOC Nanophotocatalyst Activating Persulfate Under Visible Light for the Efficient Degradation of Typical PPCPs

LEI Qian, XU Lu, AI Wei, LI Zhi-min, YANG Lei\*

(School of Environmental and Municipal Engineering, Xi'an University of Architecture and Technology, Xi'an 710055, China)

Abstract: A new type of CDs-BOC photocatalyst was synthesized in a convenient two-step method of hydrothermal and calcination processes. Carbon quantum dots (CDs) were used to modify BiOCl nanosheets. The as-prepared nanocomposite was characterized by X-ray diffraction (XRD), scanning electron microscopy (SEM), high-resolution transmission electron microscopy (HRTEM), UV-vis diffuse reflectance spectroscopy (DRS), X-ray photoelectron spectroscopy (XPS), and photoluminescence spectroscopy (PL), which showed that CDs were successfully introduced. The absorption edge of 7% CDs-BOC nanocomposite was broadened to the visible light region (424 nm), and the charge separation efficiency was remarkably improved. To improve the degradation efficiency of organic pollutants, persulfate (PS) was also introduced into the system. Due to the excellent photocatalytic ability of the nanocatalyst, the photogenerated electrons can effectively activate the PS to produce more reactive oxidizing species (ROS). Under visible light ( $\lambda > 420$  nm) irradiation, 5 mg·L<sup>-1</sup> acetaminophen (AAP) can be completely removed within 20 min. Via radical quenching experiments and electron paramagnetic resonance spectroscopy (EPR), the major ROS are determined to be ·OH, ·SO<sub>4</sub><sup>-</sup>, ·O<sub>2</sub><sup>-</sup>, and h<sup>+</sup>, and the photodegradation mechanism is proposed. The excellent photocatalytic performance of the CDs-BOC/PS system shows broad practical potential for wastewater treatment.

Key words: visible-light photocatalysis; persulfate activation; carbon quantum dots; reactive oxidizing species; acetaminophen (AAP)

对-乙酰氨基酚(acetaminophen,AAP)作为一种常用的解热镇痛药,其已成为一种在水中被检出的典型个人药品及护理品(PPCPs)<sup>[1]</sup>.通常,人体内多数未代谢的 AAP 分子通过排泄物排出体外,然后释放到水生环境中,甚至在地表水、污水处理厂及饮用水中被检出<sup>[2,3]</sup>.由于 AAP 具有抗性分子结构,难以通过传统废水处理工艺将其充分降解,因此新型高级氧化工艺引起了研究者的关注<sup>[4]</sup>.众所周知,高级氧化工艺(AOPs)是利用活性氧化物质(ROS,例如·OH)对水中的有机微污染物进行化学氧化去除的有效方法<sup>[5,6]</sup>.近年来,硫酸根自由基(·SO<sub>4</sub><sup>-</sup>)由于其氧化电位较高(2.5~3.1 V vs. NHE),pH适用范围更广,寿命较长(30~40 µs)引起了学界的兴

趣<sup>[7]</sup>. 其可通过加热、紫外照射、过渡金属、活性炭、超声或者碳纳米管活化过氧化一硫酸盐(PMS)或过硫酸盐(PS)来生成<sup>[8]</sup>. 因此,活化过硫酸盐的新体系被认为是可以代替传统羟基自由基体系的新型高级氧化技术.

近年来,卤氧铋 BiOX(X表示 Cl、Br 和 I)作为一种新型的层状半导体光催化剂在环境修复和能量转化领域引起了广泛关注<sup>[9,10]</sup>.其中,氯氧化铋(BiOCl)因为其较宽的带隙而具有出色的光催化还

收稿日期: 2020-11-04; 修订日期: 2020-12-08

基金项目: 国家自然科学基金青年科学基金项目(51808434); 陕西省科技厅自然科学基础研究计划项目(2018JQ5129)

作者简介: 雷倩(1995~),女,硕士研究生,主要研究方向为光催化 高级氧化水处理技术,E-mail;lq19951011@163.com

\* 通信作者,E-mail:yanglei\_hj@ xauat.edu.cn

原及氧化性能<sup>[9,11~14]</sup>. 然而,较宽的带隙使得 BiOCl 仅能吸收紫外光,这严重限制了其在可见光驱动的光催化反应中的应用<sup>[14,15]</sup>. 通常采用以下 4 种方法来改善 BiOCl 的可见光吸收和光催化活性,例如异质结<sup>[16]</sup>、元素掺杂<sup>[17]</sup>、富铋<sup>[18]</sup>和引入缺陷<sup>[19,20]</sup>.

碳量子点(CDs)是一种新型碳纳米材料,因其低生物毒性,独特的光致电子转移能力而备受关注<sup>[21,22]</sup>.有研究人员将CDs引入到BiOCl光催化剂中,以实现更宽的可见光响应区域和更高的电子转移效率. Di等<sup>[23]</sup>通过溶剂热法制备了CDs改性的BiOCl,在紫外线、可见光和近红外照射下降解BPA和罗丹明B,然而整个降解过程耗时120 min. Gu等<sup>[24]</sup>采用乙二醇作溶剂,采用水热法制备的微球状CQDs@BiOCl在可见光照射下180 min 内可有效降解罗丹明B.

然而,先前的研究多采用溶剂热法制备复合催化剂,对于材料的光催化性能提升效果有限,对有机污染物的氧化降解速率较慢.本研究采用简便高效的水热-煅烧两步法制备 CDs-BOC 催化剂,利用 CDs优异的电子转移特性进行材料微结构调控,以提高复合材料的可见光响应和光致电子空穴对的分离效率,同时引入 PS 以提高反应体系内活性氧化成分的组成与产率,进而提高 CDs-BOC 的可见光催化性能.构建的 CDs-BOC/PS/Vis 体系在可见光源照射20 min 内可完全催化降解 AAP,并且探明了体系中的主要活性氧化物质,提出了该体系的降解机制,以期为光催化-过硫酸盐复合高级氧化技术在水处理方面的应用提供可行的新思路与理论依据.

#### 1 材料与方法

#### 1.1 实验试剂

主要试剂:硝酸铋[Bi(NO<sub>3</sub>)<sub>3</sub>·5H<sub>2</sub>O]、对苯醌(BQ)均为分析纯,购自麦克林;过(二)硫酸钾(PS)、氯 化钾(KCl)、尿 素、柠 檬 酸、甲 醇(MeOH)、叔丁醇(TBA)、二甲基亚砜(DMSO)和乙二胺四乙酸二钠(EDTA-2Na)均为分析纯,购自天津科密欧;实验用水为超纯水(18.25  $M\Omega \cdot cm$ ).

#### 1.2 催化剂的制备

采用水热法<sup>[21]</sup>制备 CDs:准确称取 3.0 g 柠檬酸和 1.0 g 尿素溶于 10 mL 超纯水中,然后将上述溶液转移至高压反应釜中,180℃下反应 5 h. 冷却至室温后,将混合物转移至离心管并高速离心 30 min,取上清液进行冷冻干燥.

参考前人的研究制备 BiOCl 前驱体(BOC)<sup>[25]</sup>: 将 0.2 mol 的 Bi  $(NO_3)_3 \cdot 5H_2O$ 溶解在 20 mL 的  $1 \text{ mol} \cdot L^{-1}$  HNO<sub>3</sub> 中并超声搅拌形成澄清溶液,另外

将 0.2 mol 的 KCl 溶解在 30 mL 的超纯水中. 然后将两种溶液混合形成白色悬浊液. 通过加入 NaOH (1 mol·L<sup>-1</sup>)将悬浊液的 pH 值调至 7. 随后搅拌 60 min,将混合物转移到高压反应釜中. 在 160℃下水热处理 20 h 后,冷却至室温,再依次用无水乙醇和超纯水离心洗涤,最后将沉淀物在 60℃烘箱中干燥处理.

制备 CDs-BOC 复合催化剂:准确称取 35 mg CDs 溶于 20 mL 无水乙醇,再准确称取 465 mg BiOCl 前驱体加入其中,将上述混合物置于加热磁力搅拌器于 40℃下持续搅拌直到无水乙醇全部挥发.接着将得到的粉体在空气氛围下保持 300℃煅烧 3 h,升温速率为 3℃·min<sup>-1</sup>.最终得到 7% CDs-BOC 复合纳米催化剂.此外,制备了质量分数分别为 1%、3%和 10%的 CDs-BOC,以 1CB、3CB、7CB和 10CB表示.

#### 1.3 分析测试仪器

XRD 采用布鲁克 D8 ADVANCE 型 X 射线衍射仪测试, SEM 通过 MIRA3 TESCAN 型扫描电镜拍摄, TEM 采用 JEOL JEM-2100 F 型透射电子显微镜进行测量, XPS 采用美国赛默飞 ESCALAB Xi\*X 射线光电子能谱仪, 紫外可见漫反射吸收光谱采用 PE Lambda950 UV-VIS-NIR 光谱仪测试, PL 采用爱丁堡 FLS1000 瞬态稳态光谱仪进行测量.

采用美国赛默飞生产的 U3000 型超高效液相 色谱仪检测降解过程中 AAP 的浓度变化,使用赛默飞 C18 色谱柱进行分离,乙腈和纯水作为流动相,其比例为 30:70,检测波长为 243 nm;采用德国布鲁克公司生产的 ZMXmicro-6/1 型电子顺磁共振波谱仪检测体系中产生的自由基;通过马尔文-ZS90型号的 ZETA 电位仪测定催化剂在不同 pH 环境下的表面带电性.

#### 1.4 光催化性能评估

AAP 降解实验在具有冷却水循环系统的 250 mL 双层玻璃容器中进行. 采用具有 420 nm 截止滤光片的 300 W Xe 灯用作可见光光源. 通过太阳能功率计测量反应溶液表面的光强度为(2 100 + 10) W·m<sup>-2</sup>. 每次实验将 50 mg 催化剂投加到 50 mL AAP 浓度为 5 mg·L<sup>-1</sup>的反应溶液中,并在黑暗中搅拌 30 min 以确保体系达到吸附-解吸平衡. 然后,在光照射之前将向悬浮液中添加一定浓度 PS. 光催化反应期间,每隔一定时间段提取 1 mL 悬浮液,并通过 0. 22 μm 滤膜过滤进行下一步超高效液相色谱分析. 在循环实验中,将反应后的溶液离心洗涤得到催化剂,干燥处理后进行下一次实验,每次实验保证反应条件一致.

#### 2 结果与讨论

#### 2.1 催化剂表征

图 1 为 BOC 和 7CB 的 XRD 图谱,所制备材料的所有衍射峰均与 BiOCl(JCPDS 06-0249)的四方晶体结构的特征衍射峰一致,说明没有其他杂质存在. 但是,在 21.5°处 CDs 的特征峰较弱,以致于在7CB 中观察不到,这主要是由于复合物中 CDs 的含量非常低[26]. 此外,与纯 BOC 相比,复合材料的衍射峰未发生明显位移,说明引入 CDs 并未改变复合纳米催化剂的晶相和结构.

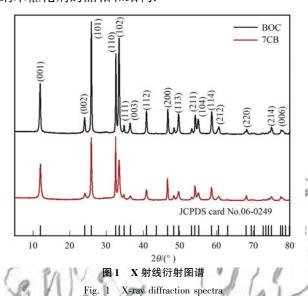


图 2 展示了所制备催化剂的微观形貌. 从 BOC 的扫描电镜图 2 (a)可看出 BOC 样品是由形状圆润

且光滑的纳米片紧密堆积而成. 图 2 (b)显示复合催化剂为直径大约 200 nm 的纳米薄片结构,通过HRTEM 进一步观察,在图 2 (c)中分布着一些直径大约 2~3 nm 的纳米点,这代表碳量子点已经结合在 BOC 表面<sup>[23,27]</sup>. 在图 2 (d)中可以观察到与 BOC (101)晶面间距对应的 0. 331 nm 晶格条纹,而周围 0. 326 nm 的晶格条纹则与 CDs 的(002)晶面间距一致<sup>[24,28,29]</sup>. 这一结果说明 CDs 已经成功地附着在 BOC 纳米片表面.

如图 3 所示,通过紫外可见漫反射法评估了复 合材料的光吸收特性. BOC 的光吸收边界大约为 358 nm, 而在引入 CDs 之后的 7CB 光吸收边界被扩 宽到 424 nm 附近并且出现吸收尾峰,延伸至大部分 可见光区域,表明复合材料具有较好的可见光响应, 这意味着在相同强度的可见光照射下,7CB可以被 光子激发产生更多的电子空穴对,进而增强光催化 效应. 通过 Kubelka-Munk 公式: $E_s = 1240/\lambda_s$ (其中 λ<sub>s</sub> 表示光吸收边界) 计算可得到催化剂的带隙 能[30], BOC 和 7CB 的带隙能分别为 3.46 eV 和 2.92 eV. 可见 CDs 的掺入可以略微缩小材料的带隙 能,但因为引入的 CDs 含量很小,所以复合催化剂 依然保持着 BOC 的晶体结构. 通常半导体的掺杂改 性会导致其结构和组成发生变化,进而影响材料的 电子结构和光吸收特性.此外,材料表面的掺杂可在 衬底材料的带隙中产生掺杂能级,从而增加光吸收 尾峰[24,31].

PL强度越高意味着电子空穴对的复合率越

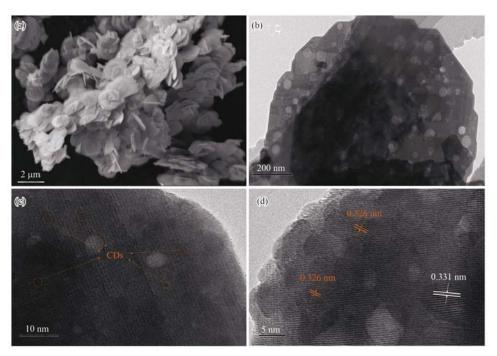


图 2 BOC 的 SEM 图像以及 7CB 的 TEM 和 HRTEM 图像

Fig. 2 SEM image of BOC, TEM, and HRTEM images of 7CB

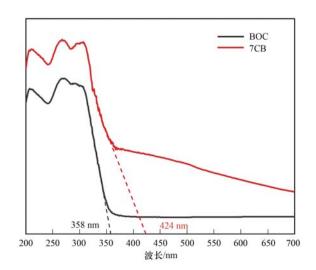
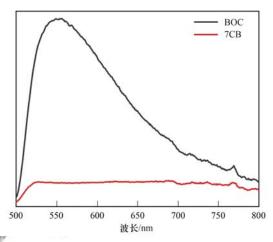


图 3 紫外-可见漫反射吸收光谱图

Fig. 3 UV-Vis diffuse reflectance spectra



高<sup>[23]</sup>. 从图 4 稳态荧光光谱可以看出,在 470 nm 的激发波长下,BOC 和 7CB 均在 550 nm 处出现发射峰,但 7CB 的发射峰强度远小于 BOC,这表明引入CDs 抑制了光致电子空穴对的复合. 由于两种材料间能级匹配使得光致电子可以由 BOC 导带注入到CDs 表面,而电子注入发生在 fs ~ ps 时域,此电子转移反应的速率远远快于载流子复合<sup>[30]</sup>. 荧光衰减越快表明电子更有效地转移,即电子空穴对的分离效率越高<sup>[4,32]</sup>. 故而对于 CDs-BOC 复合材料,荧光寿命越短代表其电子空穴对的分离效率越高. 通过对瞬态荧光光谱数据进行双指数拟合,计算得到的BOC 和 7CB 的 PL 衰减时间常数( $\tau_A$ )分别为 1.054 ns 和 0.927 ns(表 1). 显然,7CB 的  $\tau_A$  较短,这进一步证明了界面电荷转移有助于电荷分离,进而提高了光催化剂的催化活性.

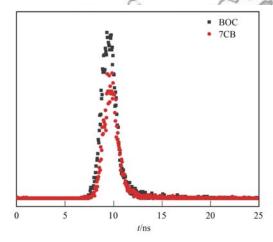


图 4 BOC 和 7CB 的稳态荧光光谱和瞬态荧光光谱

Fig. 4 Steady state fluorescence spectrum and transient fluorescence spectrum of BOC and 7CB

表 1 衰减时间常数计算

样品

BOC

7CB

rabie i	Carculation of	attenuation	time constants		
$B_1/\%$	$ au_1/\mathrm{ns}$	$B_2/\%$	$ au_2/\mathrm{ns}$	$ au_{ m A}/{ m ns}$	
281. 626	0. 762 0	0.715	9. 879 9	1. 054	_
164 016	0 629 7	1 426	5 140 0	0.027	

 $\tau_A$ 由公式(1) 计算,其中  $\tau_i$  表示 i 指数拟合的 衰减寿命, $B_i$  表示相应的占比:

$$\tau_{\rm A} = \sum_{i=1,2,3} B_i \tau_i^2 / \sum_{i=1,2,3} B_i \tau_i \tag{1}$$

为了更进一步研究复合催化剂的化学组成和价态以及电子转移效率,进行了 X 射线光电子能谱(XPS)测试. 如图 5 所示,BOC 和 7CB 的总谱图[以 C 1s(284.6eV)为基准校正]包含了 Bi、Cl、O 和 C 这 4 种元素,与其结构式一致. 在高分辨图谱中(图 6),O 1s 在 530.0 eV 和 531.3 eV 处出现两个峰,分别对应于 Bi—O 和氧空位<sup>[33]</sup>. 这里少量的氧空位主要来自制备过程中自然产生的缺陷. 从 Cl 2p 的 XPS 谱图,可以看到拟合出两个结合能位于 197.9 eV 和

199. 5 eV 的峰,分别对应 Cl  $2p_{3/2}$ 和 Cl  $2p_{1/2}$  [2]. Bi 4f 的图谱中存在两个不同结合能的特征峰,分别对应 Bi  $4f_{7/2}$  (159. 1 eV)和 Bi  $4f_{5/2}$  (164. 5 eV),具有 5. 4 eV 的分裂能,表明 Bi 以 Bi<sup>3+</sup>的形式存在于样品中,这与相关研究的报道一致<sup>[23,24]</sup>. 在 C 1s 图谱中,可以看到有 3 个结合能不同的拟合峰,分别归因于 C—C/C = C (284. 8 eV)、C—O (286. 2 eV)和 C = O(288. 3 eV),表明 CDs 成功结合在 BiOCl 表面 [21,26,34~36]. XPS 结果说明了 CDs 和 BiOCl 共存于7CB 催化剂中,证实了复合材料的成功组合.

#### 2.2 可见光催化活性评价及其机制分析

为研究 CDs-BOC 的光催化性能,采用 AAP 为目标污染物(底物),为了清楚地说明 AAP 降解过程的动力学,使用伪一级反应速率表达[式(2)]来比较不同体系的反应速率<sup>[21]</sup>:

$$-\ln(c_t/c_0) = k_{app}t \tag{2}$$

式中 $,c_{\iota}$ 代表t时刻的反应溶液中的底物浓度 $,c_{0}$ 代

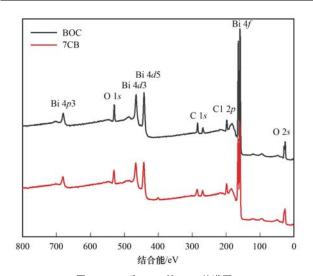


图 5 BOC 和 7CB 的 XPS 总谱图

Fig. 5 XPS survey spectra of BOC and 7CB

表初始反应溶液中底物浓度, $k_{app}$ 为表观反应速率常数.

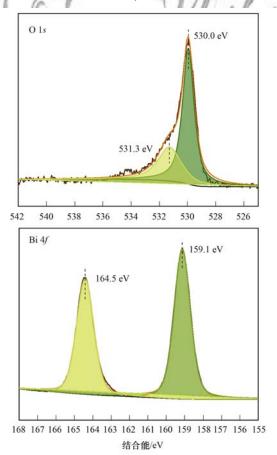
#### 2.2.1 CDs-BOC/PS 体系的可光催化性能评价

由图 7 可以看出,在可见光照射下,PS 几乎不能降解 AAP,说明可见光不能激活 PS. 在黑暗条件下,由于 7CB 材料的吸附效果,仅有 2.5%的 AAP被吸附去除.此外,BOC/PS 体系在光照射 20 min后,仅降解了 16.2%的 AAP,从 UV-vis DRS 和 PL

分析可知,这是因为 BOC 具有较宽的带隙和较高的 光致电子-空穴对复合率,所以限制了该体系对 AAP 的降解. 引入 CDs 之后, CDs-BOC/PS 体系明显具有 更高的 AAP 去除效率. 这是因为 CDs 具有优异的电 子转移特性,可以将 BOC 产生的光生电子转移至材 料表面,进一步激活溶液中的PS产生·SO4,从而提 高了电子空穴对的利用效率,此外,未被激活的 PS 可与H,O反应生成·OH和·O,,,增加了体系中的活 性氧化物质[30,37]. AAP 的降解效率随着 CDs 掺杂比 例的升高而增加, 当 CDs 的比例从 1% 提高到 10% 时, AAP 的去除率分别从 60.1% 提升至 95.6% 甚至 99%. 然而, 当 CDs 的比例从 7% 增加到 10%, 10CB/PS 的降解速率略有下降,这是因为过多的 CDs 会和 BOC 竞争吸收光子并为光生电子空穴对 提供复合位点[21,38,39]. 在不添加 PS 时,7CB 在光照 20 min 对 AAP 的降解率只有 59%,降解速率也远远 低于7CB/PS体系,这说明CDs和BOC的复合更有 利于激活 PS,从而大幅提升体系的光催化效率.

#### 2.2.2 反应条件对光催化降解 AAP 的影响

反应溶液的初始底物浓度显著影响着降解效率. 如图 8 所示,随着反应溶液中 AAP 的浓度从 2.5  $mg \cdot L^{-1}$ 增加到 20  $mg \cdot L^{-1}$ , AAP 降解效率从 99.2%



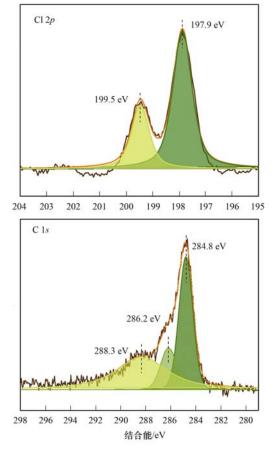
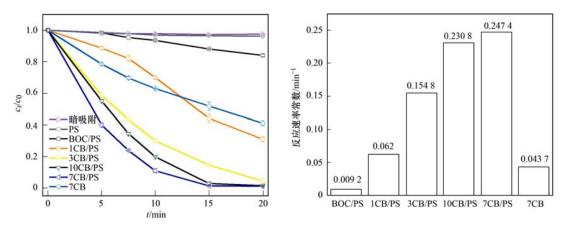


图 6 7CB的O1s、Cl2p、Bi4f和C1s XPS谱图

Fig. 6 O 1s, Cl 2p, Bi 4f, and C 1s XPS spectrum of 7CB



实验条件:催化剂投加量为 1.0 g·L<sup>-1</sup>; AAP 浓度为 5 mg·L<sup>-1</sup>; PS 浓度为 2 mmol·L<sup>-1</sup>; 光照强度为(2 100 + 10) W·m<sup>-2</sup> **图 7** 不同体系和 CDs 掺杂比例对 AAP 降解效率的影响

Fig. 7 Effects of different systems and CDs doping ratios on AAP degradation efficiency

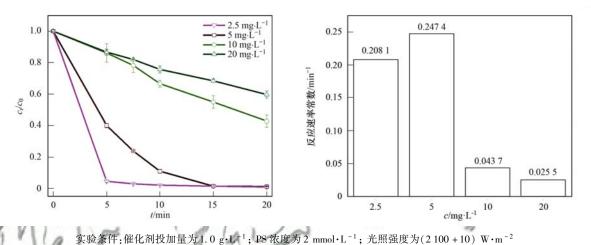


图 8 反应溶液初始底物浓度对降解效率的影响

Fig. 8 Effect of initial concentration of reaction solution on degradation efficiency

降低到 40.5%,降解反应速率常数也明显随着反应溶液浓度的增加从 0.2474 min<sup>-1</sup>急剧下降到 0.0255 min<sup>-1</sup>.这主要是由于当催化剂和 PS 投加量一定时,所产生的光生电子空穴对和活性氧化物质的数量也是一定的.当 AAP 的浓度足够低时,7CB/PS 体系产生的活性氧化物质可以充分地氧化 AAP 分子,而随着 AAP 浓度的增加,体系中的活性氧化物质便会相对地逐渐减少,这就导致了反应速率和降解效率的下降.同时,降解 AAP 过程中产生的中间产物也会消耗一定的活性氧化物质,与 AAP 分子形成竞争关系,所以高底物浓度下反应速率会明显降低.

如图 9 所示,随着催化剂浓度从 0. 25 g·L<sup>-1</sup> 增加到 1. 2 g·L<sup>-1</sup>, AAP 的降解效率从 54. 0%增加到 100%,反应速率也随着催化剂投加量的增加而增加. 这是因为随着催化剂投加量的增多,单位时间内催化剂能捕获更多光子,从而生成更多光致电子空穴对,转移到 CDs 表面的大量自由电子进而与 PS和 0<sub>2</sub> 反应生成更多活性氧化物质.同时,催化剂表

面的反应活性位点增多,更容易接触到 AAP 分子,进而提高了 AAP 降解效率和反应速率. 然而,当催化剂浓度从1.0 g·L<sup>-1</sup>增加到1.2 g·L<sup>-1</sup>时,相应的降解效率和反应速率并没有得到太大幅度地提升,这是由于体系中的 PS 用量一定,其生成的活性氧化物质是有限的,因此限制了反应速率的进一步提升.

PS 的用量在该可见光催化体系中起着十分重要的作用. 从图 10 观察到,当反应溶液中的 PS 浓度从 1 mmol·L<sup>-1</sup>增加到 4 mmol·L<sup>-1</sup>, AAP 的去除效率从 88. 1%增加到 100%,相应地表观反应速率常数也从 0. 197 9 min<sup>-1</sup>逐渐升高到 0. 450 4 min<sup>-1</sup>. 这说明在可见光催化体系中引入 PS 有利于提高整体的光催化降解效率. 但是,当 PS 浓度从 3 mmol·L<sup>-1</sup>增加到 4 mmol·L<sup>-1</sup>, AAP 的去除效果并没有明显提升,这是因为当 PS 浓度越来越高时,体系中的催化剂用量成为降解反应的主要限制因素,没有足够的自由电子去激活 PS. 并且,失活的 PS 会与·SO<sub>4</sub> 发生反应[式(3)],导致活性氧化物质减少,从而一定

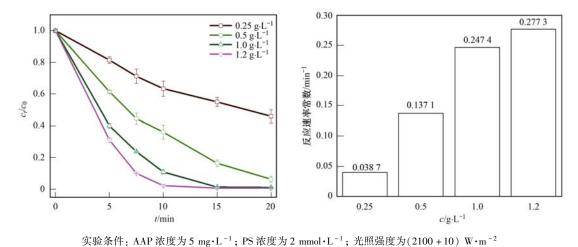
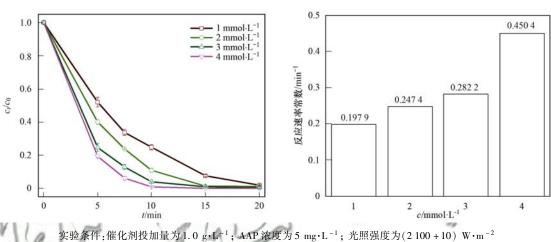


图 9 催化剂浓度对降解的影响





#### 图 10 PS 用量对降解的影响

Fig. 10 Effect of PS dosage on degradation

程度上降低了 AAP 的光催化氧化反应速率<sup>[40,41]</sup>. 这 表明,适量地加入 PS 会提高体系的光催化活性.

$$HSO_5^- + \cdot SO_4^- = SO_5^- \cdot + SO_4^{2-} + H^+$$
 (3)

初始溶液 pH 值是另一个影响降解反应的重要 因素. 通过添加 0.1 mol·L<sup>-1</sup>的 NaOH 和 HCl 调节反 应溶液的 pH 值,图 11 展示了不同 pH 时 7CB 表面 Zeta 电位和 AAP 降解效率变化结果. 在酸性或中性 条件下的降解效率明显优于碱性条件,当 pH 值从 3 升高到 10, AAP 的去除率从 99% 减少到 88.4%, 反 应速率也相应地下降. 这是由于在不同的 pH 条件 下,AAP、PS 和催化剂表面带有不同的电荷,AAP 和 PS 的 pK<sub>a</sub> 分别为 9.5 和 9.4<sup>[42,43]</sup>,即当 pH 增大 到 9.6, AAP 开始解离为负离子, 同时 PS 开始以大 量的 HSO; 形式存在. 结合 7CB 表面 Zeta 电位结果 来看,当 pH 在 3~11 范围内时,材料表面带负电 荷,当pH小于9.6,AAP和PS都带正电荷,由于库 仑引力作用使得材料表面更容易吸附 AAP 和 PS, 有利于自由电子激活 PS 以产生 ROS 氧化 AAP 分 子. 相反地, 当 pH 增大到 11, AAP 和 PS 由于解离成 离子而带负电,与催化剂表面形成库仑斥力,阻碍了 彼此之间的接触,从而导致降解效率的降低,除此之 外,部分·SO<sub>4</sub>会与 OH - 反应生成寿命较短且氧化 电位相对较低的·OH[式(4)][4,44],因此,高浓度的 OH<sup>-</sup>会消耗部分·SO<sub>4</sub>,进而降低 AAP 的氧化反应 速率.

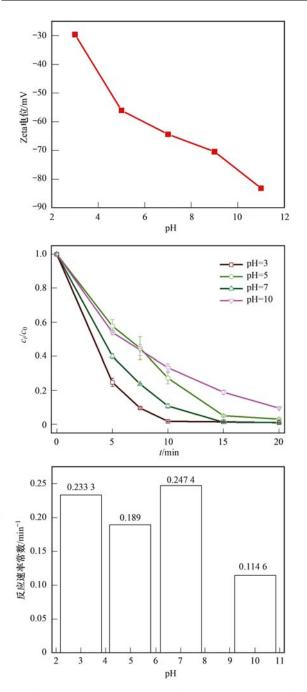
$$\cdot SO_4^- + OH^- \longrightarrow SO_4^{2-} + \cdot OH \tag{4}$$

#### 2.3 催化剂循环利用实验

为了研究复合催化剂的稳定性,通过对回收材 料进行离心和干燥的方法进行了5个循环实验,实 验中催化剂浓度、污染物浓度和 PS 用量保持不变. 结果如图 12 所示,经过 5 个连续循环实验后, AAP 的降解效率从99%略微下降到98.2%,几乎没有变 化,显示了7CB 复合纳米催化剂具有优异的理化稳 定性和可回收利用性.

#### 2.4 活性氧化物质的确定

为了探究 7CB/PS 可见光催化体系对 AAP 降 解的反应机制,利用自由基淬灭实验来确定体系的

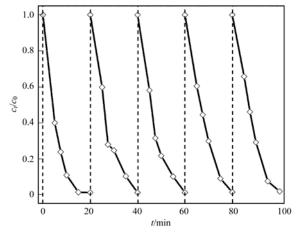


实验条件:催化剂投加量为 1.0 g·L<sup>-1</sup>; AAP 浓度为 5 mg·L<sup>-1</sup>; PS 浓度为 2 mmol·L<sup>-1</sup>; 光照强度为(2 100 + 10) W·m<sup>-2</sup>

#### 图 11 7CB 在不同 pH 值下的 Zeta 电位和 初始溶液 pH 值对降解的影响

Fig. 11 Zeta potential of 7CB catalyst at different pH values and the effect of initial solution pH on degradation

主要活性氧化物质. 通常,采用乙二胺四乙酸二钠 (EDTA-2Na)作为空穴( $h^+$ )淬灭剂,对苯醌(BQ)作为  $\cdot$  O<sub>2</sub> 的淬灭剂,甲醇(MeOH)淬灭  $\cdot$  OH和  $\cdot$  SO<sub>4</sub> ,叔 丁醇(TBA)淬灭  $\cdot$  OH $^{[4,30,45]}$ . 本实验中 BQ 和 EDTA-2Na 的浓度均为 0.5 mmol  $\cdot$  L $^{-1}$ , MeOH 和 TBA 与 PS 的量比均为1 000: 1. 结果如图 13 所示,加入不同 的淬灭剂后,降解效率和反应速率相较于空白组都 有所下降,其中 BQ 对反应体系的抑制效果最突出,



实验条件:催化剂投加量为 1.0 g·L<sup>-1</sup>; AAP 浓度为 5 mg·L<sup>-1</sup>; PS 浓度为 2 mmol·L<sup>-1</sup>; 光照强度为(2100 + 10) W·m<sup>-2</sup> 图 12 7CB 催化剂循环利用实验

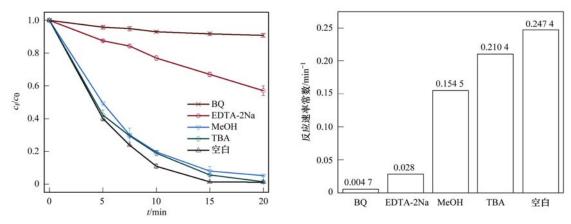
#### Fig. 12 Experiment on recycling the 7CB catalyst

使得 AAP 的去除率下降了 10 倍仅存 9. 2%. 其次是 EDTA-2Na 的抑制效果较为明显, AAP 的降解效率 从 99% 下降到 42. 9%. 加入 MeOH 和 TBA 后反应 速率常数分别下降到 0. 154 5  $\min^{-1}$  和 0. 210 4  $\min^{-1}$ ,降解效率略微下降. 这是因为 PS 可以与  $H_2O$  反应生成  $\cdot O_2^-$ ,同时电子与  $O_2$  反应也可以生成  $\cdot O_2^{-[46,47]}$ ,所以 BQ 的抑制效果最明显. 这一结果 说明了体系中存在的主要活性氧化物质是  $\cdot O_2^-$ 、 $h^+$ 、 $\cdot OH和 \cdot SO_4^-$ .

为了进一步验证体系中这些自由基的存在,通过电子顺磁共振(EPR)波谱仪对自由基进行直接测定.5,5-二甲基-1-吡咯啉-N-氧化物(DMPO)可以与自由基反应生成加合物以固定自由基,在超纯水中捕获·OH和·SO<sub>4</sub>,在非质子溶剂(DMSO)中检测·O<sub>2</sub>-[48].结果如图 14 所示,在黑暗条件下未观察到任何自由基信号,但在可见光照射 20 min 内出现了DMPO-·OH(强度比为1:2:2:1)和 DMPO-·SO<sub>4</sub>(强度比为1:1:1:1:1)[37]加合物的特征峰信号,证实了在光催化过程中体系产生了·OH和·SO<sub>4</sub>.并且,在光照射下观察到 DMPO-·O<sub>2</sub> 的强度比为1:1:1:1的特征峰[45],证明了 7CB/PS 光催化体系存在·O<sub>7</sub>.

#### 2.5 光催化降解机制

基于以上实验结果,提出了7CB/PS 体系在可见光照射下对 AAP 的降解机制(图 15). 引入 CDs 可以提高复合材料的可见光响应,随后 BOC 被光子激发产生光致电子空穴对,由于 CDs 的电子转移特性,光致电子被转移到 CDs 表面,激活了材料表面吸附的 PS[式(5)~(6)],产生的·SO<sub>4</sub><sup>-</sup>可以将 H<sub>2</sub>O氧化成·OH[式(10)]<sup>[45]</sup>,同时自由电子将水中的



实验条件:催化剂投加量为 1.0 g·L<sup>-1</sup>; AAP 浓度为 5 mg·L<sup>-1</sup>; PS 浓度为 2 mmol·L<sup>-1</sup>; 光照强度为(2100 + 10) W·m<sup>-2</sup> **图 13** 自由基淬灭剂对 AAP 降解效率的影响

Fig. 13 Effect of quencher on the degradation efficiency of AAP

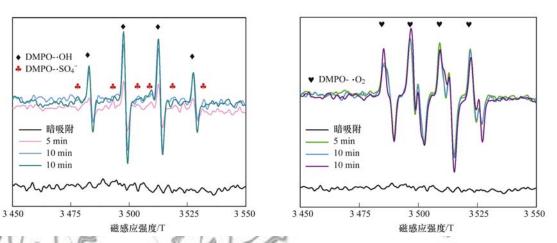


图 14 DMPO-·OH/·SO<sub>4</sub> 及 DMPO-·O<sub>2</sub> EPR 谱图

Fig. 14 EPR spectra of DMPO-·OH/·SO<sub>4</sub> and DMPO-·O<sub>2</sub>

 $O_2$  还原为 $\cdot O_2^-$ [式(7)]<sup>[30]</sup>. 此外,还有部分未被激活的 PS 与水反应生成 $\cdot O_2^-$ [式(8)~(9)]<sup>[46,47]</sup>. 这些活性氧化物质和 BOC 价带上的  $h^+$ 都具有很强的氧化性,能将 AAP 氧化降解为有机小分子进而矿化成  $CO_2$  和  $H_2O[$ 式(11)].

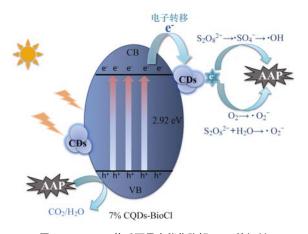


图 15 7CB/PS 体系可见光催化降解 AAP 的机制

Fig. 15 Mechanism of visible light photocatalytic degradation of AAP in the 7CB/PS system

$$7CB + hv \longrightarrow h^+ + e^- \tag{5}$$

$$e^{-} + S_2 O_8^{2-} \longrightarrow \cdot SO_4^{-} + SO_4^{2-}$$
 (6)

$$e^{-} + O_2 \longrightarrow \cdot O_2^{-} \tag{7}$$

$$S_2O_8^{2-} + 2H_2O \longrightarrow HO_2^- + 2SO_4^{2-} + 3H^+$$
 (8)

$$HO_2^- + S_2O_8^{2-} \longrightarrow \cdot SO_4^- + SO_4^{2-} + H^+ + \cdot O_2^-$$
 (9)

$$\cdot SO_4^- + H_2O \longrightarrow \cdot OH \tag{10}$$

$$h^+/\cdot O_2^-/\cdot SO_4^-/\cdot OH + AAP \longrightarrow CO_2 + H_2O$$
 (11)

#### 3 结论

- (1)通过简便高效的水热-煅烧两步法成功地合成了 CDs-BOC 复合纳米催化剂,物化和光学表征结果证明了 CDs 的成功引入,并显著提升了材料对可见光的吸收效率和光致电子空穴对的分离效率.
- (2)通过降解 AAP 评估了复合催化剂的光催化性能,发现引入 CDs 可明显提高光催化剂对 AAP 的降解效率. 此外,加入 PS 后,AAP 的降解速率提高了 6 倍,且在 20 min 内几乎被完全降解. 循环实验证明了材料良好的理化稳定性和潜在的应用价值.
  - (3)自由基淬灭实验和电子顺磁共振测试结果

- 表明:  $\cdot O_2^-$ 、光生空穴( $h^+$ )、 $\cdot OH$  和  $\cdot SO_4^-$ 为7CB/PS/Vis体系的主要活性氧化物质.
- (4)提出了 7CB/PS/Vis 体系降解 AAP 的机制,由于引入的 CDs 具有优异的电子转移特性,提高了复合材料光致电子空穴对的利用率,展现了 CDs-BOC/PS 可见光催化体系降解水中有机污染物的优异性能和应用潜力.

#### 参考文献:

- [ 1 ] González-Pleiter M, Gonzalo S, Rodea-Palomares I, et al.

  Toxicity of five antibiotics and their mixtures towards photosynthetic aquatic organisms; implications for environmental risk assessment [ J ]. Water Research, 2013, 47 (6): 2050-2064.
- [ 2 ] Zhang X, Wang X B, Wang L W, et al. Synthesis of a highly efficient BiOCl single-crystal nanodisk photocatalyst with exposing {001} facets[J]. ACS Applied Materials & Interfaces, 2014, 6 (10): 7766-7772.
- [ 3 ] Bean T G, Rattner B A, Lazarus R S, et al. Pharmaceuticals in water, fish and osprey nestlings in Delaware River and Bay[J]. Environmental Pollution, 2018, 232: 533-545.
- [4] Du X Y, Bai X, Xu L, et al. Visible-light activation of persulfate by TiO<sub>2</sub>/g-C<sub>3</sub>N<sub>4</sub> photocatalyst toward efficient degradation of micropollutants [J]. Chemical Engineering Journal, 2020, 384, doi: 10.1016/j.cej.2019.123245.
- [5] Hodges B C, Cates E L, Kim J H. Challenges and prospects of advanced oxidation water treatment processes using catalytic nanomaterials[J]. Nature Nanotechnology, 2018, 13(8): 642-650.
- [6] Hu P D, Long M C. Cobalt-catalyzed sulfate radical-based advanced oxidation: a review on heterogeneous catalysts and applications [J]. Applied Catalysis B: Environmental, 2016, 181: 103-117.
- [7] Huang G X, Wang C Y, Yang C W, et al. Degradation of bisphenol a by peroxymonosulfate catalytically activated with Mn<sub>1.8</sub> Fe<sub>1.2</sub>O<sub>4</sub> nanospheres; synergism between Mn and Fe[J]. Environmental Science & Technology, 2017, 51 (21): 12611-12618.
- [8] 赵文莉, 王广智, 弋凡, 等. 过硫酸盐活化技术的研究进展 [J]. 现代化工, 2018, **38**(7): 53-56.

  Zhao W L, Wang G Z, Yi F, *et al.* Research progress on persulfate activation technology [J]. Modern Chemical Industry, 2018, **38**(7): 53-56.
- [9] Cheng H F, Huang B B, Dai Y. Engineering BiOX (X = Cl, Br, I) nanostructures for highly efficient photocatalytic applications [J]. Nanoscale, 2014, 6(4): 2009-2026.
- [10] Ye L Q, Su Y R, Jin X L, et al. Recent advances in BiOX (X = Cl, Br and I) photocatalysts: synthesis, modification, facet effects and mechanisms [J]. Environmental Science: Nano, 2014, 1(2): 90-112.
- [11] Yang Y, Zhang C, Lai C, et al. BiOX (X = Cl, Br, I) photocatalytic nanomaterials: applications for fuels and environmental management [J]. Advances in Colloid and Interface Science, 2018, 254: 76-93.
- [12] Mi Y, Wen L Y, Wang Z J, et al. Fe ( III ) modified BiOCl ultrathin nanosheet towards high-efficient visible-light photocatalyst [J]. Nano Energy, 2016, 30: 109-117.
- [13] Zhao H, Liu X, Dong Y M, et al. A special synthesis of BiOCl photocatalyst for efficient pollutants removal: new insight into the

- band structure regulation and molecular oxygen activation [J]. Applied Catalysis B: Environmental, 2019, **256**, doi: 10.1016/j. apcatb. 2019. 117872.
- [14] Chen L, Yin S F, Huang R, et al. Facile synthesis of BiOCl nano-flowers of narrow band gap and their visible-light-induced photocatalytic property [J]. Catalysis Communications, 2012, 23: 54-57.
- [15] 余长林,陈建钗,操芳芳,等. Pt/BiOCl 纳米片的制备、表征及其光催化性能[J]. 催化学报, 2013, **34**(2): 385-390. Yu C L, Chen J C, Cao F F, *et al.* Preparation, characterization, and photocatalytic properties of Pt/BiOCl nanoplates[J]. Chinese Journal of Catalysis, 2013, **34**(2): 385-390.
- [16] Yu L H, Zhang X Y, Li G W, et al. Highly efficient Bi<sub>2</sub>O<sub>2</sub>CO<sub>3</sub>/BiOCl photocatalyst based on heterojunction with enhanced dye-sensitization under visible light [J]. Applied Catalysis B; Environmental, 2016, **187**; 301-309.
- [17] Wang C Y, Zhang Y J, Wang W K, et al. Enhanced photocatalytic degradation of bisphenol a by Co-doped BiOCI nanosheets under visible light irradiation [J]. Applied Catalysis B: Environmental, 2018, 221: 320-328.
- [18] Ning S B, Ding L Y, Lin Z G, et al. One-pot fabrication of Bi<sub>3</sub>O<sub>4</sub>Cl/BiOCl plate-on-plate heterojunction with enhanced visible-light photocatalytic activity [J]. Applied Catalysis B: Environmental, 2016, 185; 203-212.
- [19] Wu S J, Xiong J W, Sun J G, et al. Hydroxyl-dependent evolution of oxygen vacancies enables the regeneration of BiOCl photocatalyst[J]. ACS Applied Materials & Interfaces, 2017, 9 (19): 16620-16626.
- [20] Cui D D, Wang L, Xu K, et al. Band-gap engineering of BiOCl with oxygen vacancies for efficient photooxidation properties under visible-light irradiation [J]. Journal of Materials Chemistry A, 2018, 6(5): 2193-2199.
- [21] Xu L, Bai X, Guo L K, et al. Facial fabrication of carbon quantum dots (CDs)-modified N-TiO<sub>2-x</sub> nanocomposite for the efficient photoreduction of Cr(VI) under visible light [J]. Chemical Engineering Journal, 2019, 357; 473-486.
- [22] Zhu C, Liu C A, Zhou Y J, et al. Carbon dots enhance the stability of CdS for visible-light-driven overall water splitting[J]. Applied Catalysis B: Environmental, 2017, 216: 114-121.
- [23] Di J, Xia J X, Ji M X, et al. Carbon quantum dots modified BiOCl ultrathin nanosheets with enhanced molecular oxygen activation ability for broad spectrum photocatalytic properties and mechanism insight [J]. ACS Applied Materials & Interfaces, 2015, 7(36): 20111-20123.
- [24] Gu X S, Yan Q T, Wei Y, et al. Visible-light-responsive photocatalyst with a microsphere structure: preparation and photocatalytic performance of CQDs @ BiOCl [J]. Journal of Materials Science: Materials in Electronics, 2019, 30 (17): 16321-16336.
- [25] Chen G H, Chen G L, Wang Y, et al. Facile synthesis of N-doped BiOCl photocatalyst by an ethylenediamine-assisted hydrothermal method[J]. Journal of Nanomaterials, 2015, doi: 10.1155/2015/316057.
- [26] Li Y R, Liu Z M, Wu Y C, et al. Carbon dots-TiO<sub>2</sub> nanosheets composites for photoreduction of Cr( VI) under sunlight illumination: favorable role of carbon dots[J]. Applied Catalysis B: Environmental, 2018, 224: 508-517.
- [27] 李玲玲, 倪刚, 王嘉楠, 等. BiOCL/CQDs 复合催化剂的制备 及光催化性能研究 [J]. 功能材料, 2016, 47(4): 4134-4138.

- Li L L, Ni G, Wang J N, et al. Study on the synthesis and photocatalytic activity of BiOCl/CQDs complex photocatalysts [J]. Journal of Functional Materials, 2016, 47 (4): 4134-4138.
- [28] Zhang Z H, Huang H R, Cheng K, et al. High efficient carbon quantum dots/BiOCl nanocomposite for photocatalytic pollutant degradation[J]. Journal of Inorganic Materials, 2020, 35(4): 491-496.
- [29] Zhang Q X, Chen P, Zhuo M H, et al. Degradation of indometacin by simulated sunlight activated CDs-loaded BiPO<sub>4</sub>photocatalyst: roles of oxidative species [J]. Applied Catalysis B: Environmental, 2018, 221: 129-139.
- [30] Yang L, Bai X, Shi J, et al. Quasi-full-visible-light absorption by D35-TiO<sub>2</sub>/g-C<sub>3</sub>N<sub>4</sub> for synergistic persulfate activation towards efficient photodegradation of micropollutants [J]. Applied Catalysis B: Environmental, 2019, 256, doi: 10. 1016/j. apcatb. 2019. 117759.
- [31] Di J, Xia J X, Chen X L, et al. Tunable oxygen activation induced by oxygen defects in nitrogen doped carbon quantum dots for sustainable boosting photocatalysis[J]. Carbon, 2017, 114: 601-607.
- [32] Xu L, Yang L, Johansson E M J, et al. Photocatalytic activity and mechanism of bisphenol a removal over TiO<sub>2=x</sub>/rGO nanocomposite driven by visible light[J]. Chemical Engineering Journal, 2018, **350**: 1043-1055.
- [33] Wang H, Yong D Y, Chen S C, et al. Oxygen-vacancy-mediated exciton dissociation in BiOBr for boosting charge-carrier-involved molecular oxygen activation [J]. Journal of the American Chemical Society, 2018, 140(5): 1760-1766.
- [34] Qu X F, Liu M H, Yang J Y, et al. A novel ternary TiO<sub>2</sub>/CQDs/BiOX (X = Cl, Br, I) heterostructure as photocatalyst for water purification under solar irradiation [J]. Journal of Solid State Chemistry, 2018, 264: 77-85.
- [35] Qiu B C, Zhou Y, Ma Y F, et al. Facile synthesis of the Ti<sup>3+</sup> self-doped TiO<sub>2</sub>-graphene nanosheet composites with enhanced photocatalysis[J]. Scientific Reports, 2015, 5, doi: 10.1038/srep08591.
- [36] Chen Y, Lu Q J, Yan X L, et al. Enhanced photocatalytic activity of the carbon quantum dot-modified BiOI microsphere [J]. Nanoscale Research Letters, 2016, 11 (1), doi: 10. 1186/s11671-016-1262-7.
- [37] Wang Y P, Liu C, Zhang Y T, et al. Sulfate radical-based photo-Fenton reaction derived by CuBi<sub>2</sub>O<sub>4</sub> and its composites with α-Bi<sub>2</sub>O<sub>3</sub> under visible light irradiation: catalyst fabrication, performance and reaction mechanism [J]. Applied Catalysis B: Environmental, 2018, 235: 264-273.

- [38] Mirtchev P, Henderson E J, Soheilnia N, et al. Solution phase synthesis of carbon quantum dots as sensitizers for nanocrystalline TiO<sub>2</sub> solar cells [J]. Journal of Materials Chemistry, 2012, 22: 1265-1269.
- [39] Pan J Q, Sheng Y Z, Zhang J X, et al. Preparation of carbon quantum dots/TiO<sub>2</sub> nanotubes composites and their visible light catalytic applications [J]. Journal of Materials Chemistry A, 2014, 2(42): 18082-18086.
- [40] Gong Y, Zhao X, Zhang H, et al. MOF-derived nitrogen doped carbon modified g-C<sub>3</sub>N<sub>4</sub> heterostructure composite with enhanced photocatalytic activity for bisphenol a degradation with peroxymonosulfate under visible light irradiation [J]. Applied Catalysis B; Environmental, 2018, 233; 35-45.
- [41] Wang G L, Chen S, Quan X, et al. Enhanced activation of peroxymonosulfate by nitrogen doped porous carbon for effective removal of organic pollutants [J]. Carbon, 2017, 115: 730-739
- [42] Yang L M, Yu L E, Ray M B. Degradation of paracetamol in aqueous solutions by TiO<sub>2</sub> photocatalysis [J]. Water Research, 2008, 42(13): 3480-3488.
- [43] Hu L M, Zhang G S, Liu M, et al. Enhanced degradation of Bisphenol A (BPA) by peroxymonosulfate with Co<sub>3</sub>O<sub>4</sub>-Bi<sub>2</sub>O<sub>3</sub> catalyst activation: effects of pH, inorganic anions, and water matrix [J]. Chemical Engineering Journal, 2018, 338: 300-310.
- [44] Hammouda S B, Zhao F P, Safaei Z, et al. Sulfate radical-mediated degradation and mineralization of bisphenol F in neutral medium by the novel magnetic Sr<sub>2</sub>CoFeO<sub>6</sub> double perovskite oxide catalyzed peroxymonosulfate: influence of co-existing chemicals and UV irradiation [J]. Applied Catalysis B: Environmental, 2018, 233: 99-111.
- [45] Xu L, Yang L, Bai X, et al. Persulfate activation towards organic decomposition and Cr(VI) reduction achieved by a novel CQDs-TiO<sub>2-x</sub>/rGO nanocomposite [J]. Chemical Engineering Journal, 2019, 373: 238-250.
- [46] Chen X, Oh W D, Lim T T. Graphene-and CNTs-based carbocatalysts in persulfates activation; material design and catalytic mechanisms [J]. Chemical Engineering Journal, 2018, 354: 941-976.
- [47] Furman O S, Teel A L, Watts R J. Mechanism of base activation of persulfate [J]. Environmental Science & Technology, 2010, 44(16): 6423-6428.
- [48] Dai Z, Qin F, Zhao H P, et al. Crystal defect engineering of aurivillius Bi<sub>2</sub>MoO<sub>6</sub> by Ce doping for increased reactive species production in photocatalysis [J]. ACS Catalysis, 2016, 6(5): 3180-3192.

### **HUANJING KEXUE**

Environmental Science (monthly)

Vol. 42 No. 6 Jun. 15, 2021

#### **CONTENTS**

Advances and Challenges in Biosafety Research for Urban Environments · · · · · · · · · · · · · · · · · · ·	SU Jian-qiang, AN Xin-li, HU An-yi, et al. (2565)
Key Problems and Novel Strategy of Controlling Emerging Trace Organic Contaminants During Municipal Wastewater Reclamation	····· WANG Wen-long, WU Qian-yuan, DU Ye, et al. (2573)
Mechanisms Summary and Potential Analysis of EPS as a Flame Retardant	
Concentrations, Sources, and Health Risks of PM <sub>2.5</sub> Carrier Metals in the Beijing Urban Area and Suburbs	
MAIAC AOD and PM2.5 Mass Concentrations Characteristics and Correlation Analysis in Beijing-Tianjin-Hebei and Surrounding Areas	
	··· JIN Jian-nan, YANG Xing-chuan, YAN Xing, et al. (2604)
Formation and Prevention of Secondary Nitrate in PM <sub>2.5</sub> in Tianjin	
Pollution Characteristics and Risk Assessment of Nitro Polycyclic Aromatic Hydrocarbons in PM2.5 of Nanjing, China	
Spatio-temporal Patterns and Potential Sources of Absorbing Aerosols in the Fenwei Plain	
Sources Apportionment of Oxygenated Volatile Organic Compounds (OVOCs) in a Typical Southwestern Region in China During Summ	er
A Local Communication of the C	
Aqueous-phase Oxidation of Dissolved Organic Matter (DOM) from Extracts of Ambient Aerosols	
Changes and Potential Sources of Atmospheric Black Carbon Concentration in Shanghai over the Past 40 Years Based on MERRA-2 Re	Analysis Data
Spatio-Temporal Evolution Characteristics and Source Apportionment of O <sub>3</sub> and NO <sub>2</sub> in Shijiazhuang	AO Shan-shan, DUAN Tu-sen, GAO Chan-chan, et al. (2008)
Applying Photochemical Indicators to Analyze Ozone Sensitivity in Handan	NIII Vuon CHENC Shui-vuon OII Sheng-iu et al. (2011)
Spatiotemporal Distribution of Aerosol Optical Depth Based on Landsat Data in the Hinterland of the Guanzhong Basin and Its Relations	
Spanotemporar Distribution of Acrossi Optical Depth Based on Earlisa Data in the Trimertand of the Quantitoning Basin and its rectation	ZHENG Yu-rong WANG Yu-hong ZHANG Yiu et al. (2690)
Multidimensional Verification of Anthropogenic VOCs Emissions Inventory Through Satellite Retrievals and Ground Observations	
Estimation of the SOA Formation Potential of the National Trunk Highway in Central Plains Urban Agglomeration	
Economic Benefit of Air Quality Improvement During Implementation of the Air Pollution Prevention and Control Action Plan in Beijing	
	LU Ya-ling, FAN Zhao-yang, JIANG Hong-qiang, et al. (2730)
Emission Performance Quantitative Evaluation and Application of Industrial Air Pollution Sources	
Screening and Sequencing High-risk Antibiotics in China's Water Environment Based on Ecological Risks	
China's Reuse Water Development and Utilization Potential Based on the RDA-REM Model	
Characteristic Analysis of SWAT Model Parameter Values Based on Assessment of Model Research Quality	
Sensitivity Analysis of Boundary Load Reduction in a Large Shallow Lake Water Quality Model	WANY Ya-ning, LI Yi-ping, CHENG Yue, et al. (2778)
Comparison of Available Nitrogen and Phosphorus Characteristics in the Land-Water Transition Zone of Different Watersheds and Their	Environmental Significance
Companies of Transaction and T	······ ZHU Hai, YUAN Xu-yin, YE Hong-meng, et al. (2787)
Analysis of Spatial-Temporal Variation Characteristics of Potential Non-point Source Pollution Risks in the Upper Beiyun River Basin U	sing Different Weighting Methods ·····
Characteristics of Runoff-related Total Nitrogen and Phosphorus Losses Under Long-term Fertilization and Cultivation on Purple Soil Slo	ping Croplands ·····
	WII Vice vii II Tien vong HF Bing bui (2010)
Hydrochemistry and Its Controlling Factors and Water Quality Assessment of Shallow Groundwater in the Weihe and Jinghe River Catch	ments ······ LIU Xin, XIANG Wei, SI Bing-cheng (2817)
Hydrochemistry and Its Controlling Factors and Water Quality Assessment of Shallow Groundwater in the Weihe and Jinghe River Catch Characteristics and Drivers of Dissolved Carbon Dioxide and Methane Concentrations in the Nantiaoxi River System in the Upper Reach	ments LIU Xin, XIANG Wei, SI Bing-cheng (2817) es of the Taihu Lake Basin During Summer-Autumn
Hydrochemistry and Its Controlling Factors and Water Quality Assessment of Shallow Groundwater in the Weihe and Jinghe River Catch Characteristics and Drivers of Dissolved Carbon Dioxide and Methane Concentrations in the Nantiaoxi River System in the Upper Reach	ments LIU Xin, XIANG Wei, SI Bing-cheng (2817) es of the Taihu Lake Basin During Summer-Autumn LIANG Jia-hui, TIAN Lin-lin, ZHOU Zhong-yu, et al. (2826)
Hydrochemistry and Its Controlling Factors and Water Quality Assessment of Shallow Groundwater in the Weihe and Jinghe River Catch Characteristics and Drivers of Dissolved Carbon Dioxide and Methane Concentrations in the Nantiaoxi River System in the Upper Reach  Nitrogen Distribution and Ingrenic Nitrogen Diffusion Flux in a Shallow Lake During the Low Temperature Period. A Case Study of the	ments LIU Xin, XIANG Wei, SI Bing-cheng (2817) es of the Taihu Lake Basin During Summer-Autumn LIANG Jia-hui, TIAN Lin-lin, ZHOU Zhong-yu, et al. (2826) Baiyangdian Lake
Hydrochemistry and Its Controlling Factors and Water Quality Assessment of Shallow Groundwater in the Weihe and Jinghe River Catch Characteristics and Drivers of Dissolved Carbon Dioxide and Methane Concentrations in the Nantiaoxi River System in the Upper Reach	ments ········ LIU Xin, XIANG Wei, SI Bing-cheng (2817) es of the Taihu Lake Basin During Summer-Autumn LIANG Jia-hui, TIAN Lin-lin, ZHOU Zhong-yu, et al. (2826) e Baiyangdian Lake ······ WEN Yan, SHAN Bao-qing, ZHANG Wen-qiang (2839)
Hydrochemistry and Its Controlling Factors and Water Quality Assessment of Shallow Groundwater in the Weihe and Jinghe River Cated Characteristics and Drivers of Dissolved Carbon Dioxide and Methane Concentrations in the Nantiaoxi River System in the Upper Reach  Nitrogen Distribution and Inorganic Nitrogen Diffusion Flux in a Shallow Lake During the Low Temperature Period; A Case Study of the  Effects of Sediment Microenvironment on Sedimentary Phosphorus Release Under Capping	ments LIU Xin, XIANG Wei, SI Bing-cheng (2817) es of the Taihu Lake Basin During Summer-Autumn LIANG Jia-hui, TIAN Lin-lin, ZHOU Zhong-yu, et al. (2826) e Baiyangdian Lake WEN Yan, SHAN Bao-qing, ZHANG Wen-qiang (2839) CHEN Shu-tong, LI Da-peng, XU Chu-tian, et al. (2848)
Hydrochemistry and Its Controlling Factors and Water Quality Assessment of Shallow Groundwater in the Weihe and Jinghe River Cated Characteristics and Drivers of Dissolved Carbon Dioxide and Methane Concentrations in the Nantiaoxi River System in the Upper Reach	ments LIU Xin, XIANG Wei, SI Bing-cheng (2817) es of the Taihu Lake Basin During Summer-Autumn  LIANG Jia-hui, TIAN Lin-lin, ZHOU Zhong-yu, et al. (2826) e Baiyangdian Lake WEN Yan, SHAN Bao-qing, ZHANG Wen-qiang (2839) CHEN Shu-tong, LI Da-peng, XU Chu-tian, et al. (2848) XUE Xiang-dong, YANG Chen-hao, YU Jian-lin, et al. (2856)
Hydrochemistry and Its Controlling Factors and Water Quality Assessment of Shallow Groundwater in the Weihe and Jinghe River Cated Characteristics and Drivers of Dissolved Carbon Dioxide and Methane Concentrations in the Nantiaoxi River System in the Upper Reach	ments LIU Xin, XIANG Wei, SI Bing-cheng (2817) es of the Taihu Lake Basin During Summer-Autumn  LIANG Jia-hui, TIAN Lin-lin, ZHOU Zhong-yu, et al. (2826) e Baiyangdian Lake  WEN Yan, SHAN Bao-qing, ZHANG Wen-qiang (2839)  CHEN Shu-tong, LI Da-peng, XU Chu-tian, et al. (2848) XUE Xiang-dong, YANG Chen-hao, YU Jian-lin, et al. (2856)  LING Xin, XU Hui-ping, LU Guang-hua (2868)
Hydrochemistry and Its Controlling Factors and Water Quality Assessment of Shallow Groundwater in the Weihe and Jinghe River Cated Characteristics and Drivers of Dissolved Carbon Dioxide and Methane Concentrations in the Nantiaoxi River System in the Upper Reach	ments
Hydrochemistry and Its Controlling Factors and Water Quality Assessment of Shallow Groundwater in the Weihe and Jinghe River Cated Characteristics and Drivers of Dissolved Carbon Dioxide and Methane Concentrations in the Nantiaoxi River System in the Upper Reach	ments
Hydrochemistry and Its Controlling Factors and Water Quality Assessment of Shallow Groundwater in the Weihe and Jinghe River Cated Characteristics and Drivers of Dissolved Carbon Dioxide and Methane Concentrations in the Nantiaoxi River System in the Upper Reach Nitrogen Distribution and Inorganic Nitrogen Diffusion Flux in a Shallow Lake During the Low Temperature Period; A Case Study of the Effects of Sediment Microenvironment on Sedimentary Phosphorus Release Under Capping Coadsorption of Heavy Metal and Antibiotic onto Humic Acid from Polder River Sediment Effects of Two PPCPs on Nitrification in Sediments in the Yarlung Zangbo River Wastewater Treatment Effects of Ferric-carbon Micro-electrolysis and Zeolite in Constructed Wetlands Z CDs-BOC Nanophotocatalyst Activating Persulfate Under Visible Light for the Efficient Degradation of Typical PPCPs Preparation of pg-C <sub>3</sub> N <sub>4</sub> /BiOBr/Ag Composite and Photocatalytic Degradation of Sulfamethoxazole	ments
Hydrochemistry and Its Controlling Factors and Water Quality Assessment of Shallow Groundwater in the Weihe and Jinghe River Cated Characteristics and Drivers of Dissolved Carbon Dioxide and Methane Concentrations in the Nantiaoxi River System in the Upper Reach Nitrogen Distribution and Inorganic Nitrogen Diffusion Flux in a Shallow Lake During the Low Temperature Period; A Case Study of the Selfects of Sediment Microenvironment on Sedimentary Phosphorus Release Under Capping Coadsorption of Heavy Metal and Antibiotic onto Humic Acid from Polder River Sediment Effects of Two PPCPs on Nitrification in Sediments in the Yarlung Zangbo River Wastewater Treatment Effects of Ferric-carbon Micro-electrolysis and Zeolite in Constructed Wetlands Z CDs-BOC Nanophotocatalyst Activating Persulfate Under Visible Light for the Efficient Degradation of Typical PPCPs Preparation of pg-C <sub>3</sub> N <sub>4</sub> /BiOBr/Ag Composite and Photocatalytic Degradation of Sulfamethoxazole Sodium Alginate Loading of Zero-Valent Iron Sulfide for the Reduction of Cr (VI) in Water	ments LIU Xin, XIANG Wei, SI Bing-cheng (2817) es of the Taihu Lake Basin During Summer-Autumn  LIANG Jia-hui, TIAN Lin-lin, ZHOU Zhong-yu, et al. (2826) e Baiyangdian Lake  WEN Yan, SHAN Bao-qing, ZHANG Wen-qiang (2839) CHEN Shu-tong, LI Da-peng, XU Chu-tian, et al. (2848) XUE Xiang-dong, YANG Chen-hao, YU Jian-lin, et al. (2856) LING Xin, XU Hui-ping, LU Guang-hua (2868) HAO Zhong-jing, HAO Qing-ju, ZHANG Yao-yu, et al. (2875) LEI Qian, XU Lu, AI Wei, et al. (2885) YANG Li-wei, LIU Li-jun, XIA Xun-feng, et al. (2896) WANG Xu, YANG Xin-nan, HUANG Bi-juan, et al. (2908)
Hydrochemistry and Its Controlling Factors and Water Quality Assessment of Shallow Groundwater in the Weihe and Jinghe River Cated Characteristics and Drivers of Dissolved Carbon Dioxide and Methane Concentrations in the Nantiaoxi River System in the Upper Reach Nitrogen Distribution and Inorganic Nitrogen Diffusion Flux in a Shallow Lake During the Low Temperature Period; A Case Study of the Effects of Sediment Microenvironment on Sedimentary Phosphorus Release Under Capping Coadsorption of Heavy Metal and Antibiotic onto Humic Acid from Polder River Sediment Effects of Two PPCPs on Nitrification in Sediments in the Yarlung Zangbo River Wastewater Treatment Effects of Ferric-carbon Micro-electrolysis and Zeolite in Constructed Wetlands Z CDs-BOC Nanophotocatalyst Activating Persulfate Under Visible Light for the Efficient Degradation of Typical PPCPs Preparation of pg-C <sub>3</sub> N <sub>4</sub> /BiOBr/Ag Composite and Photocatalytic Degradation of Sulfamethoxazole Sodium Alginate Loading of Zero-Valent Iron Sulfide for the Reduction of Cr(VI) in Water Adsorption Mechanism of Cadmium by Superparamagnetic Nano-Fe <sub>3</sub> O <sub>4</sub> @SiO <sub>2</sub> Functionalized Materials	ments
Hydrochemistry and Its Controlling Factors and Water Quality Assessment of Shallow Groundwater in the Weihe and Jinghe River Cated Characteristics and Drivers of Dissolved Carbon Dioxide and Methane Concentrations in the Nantiaoxi River System in the Upper Reach	ments
Hydrochemistry and Its Controlling Factors and Water Quality Assessment of Shallow Groundwater in the Weihe and Jinghe River Cated Characteristics and Drivers of Dissolved Carbon Dioxide and Methane Concentrations in the Nantiaoxi River System in the Upper Reach	ments
Hydrochemistry and Its Controlling Factors and Water Quality Assessment of Shallow Groundwater in the Weihe and Jinghe River Cated Characteristics and Drivers of Dissolved Carbon Dioxide and Methane Concentrations in the Nantiaoxi River System in the Upper Reach	ments
Hydrochemistry and Its Controlling Factors and Water Quality Assessment of Shallow Groundwater in the Weihe and Jinghe River Cated Characteristics and Drivers of Dissolved Carbon Dioxide and Methane Concentrations in the Nantiaoxi River System in the Upper Reach	ments
Hydrochemistry and Its Controlling Factors and Water Quality Assessment of Shallow Groundwater in the Weihe and Jinghe River Cated Characteristics and Drivers of Dissolved Carbon Dioxide and Methane Concentrations in the Nantiaoxi River System in the Upper Reach	ments
Hydrochemistry and Its Controlling Factors and Water Quality Assessment of Shallow Groundwater in the Weihe and Jinghe River Cated Characteristics and Drivers of Dissolved Carbon Dioxide and Methane Concentrations in the Nantiaoxi River System in the Upper Reach	ments
Hydrochemistry and Its Controlling Factors and Water Quality Assessment of Shallow Groundwater in the Weihe and Jinghe River Cated Characteristics and Drivers of Dissolved Carbon Dioxide and Methane Concentrations in the Nantiaoxi River System in the Upper Reach	ments
Hydrochemistry and Its Controlling Factors and Water Quality Assessment of Shallow Groundwater in the Weihe and Jinghe River Cated Characteristics and Drivers of Dissolved Carbon Dioxide and Methane Concentrations in the Nantiaoxi River System in the Upper Reach Characteristics and Drivers of Dissolved Carbon Dioxide and Methane Concentrations in the Nantiaoxi River System in the Upper Reach Characteristics of Sediment Microenvironment on Sedimentary Phosphorus Release Under Capping Coadsorption of Heavy Metal and Antibiotic onto Humic Acid from Polder River Sediment Effects of Two PPCPs on Nitrification in Sediments in the Yarlung Zangbo River Wastewater Treatment Effects of Ferric-carbon Micro-electrolysis and Zeolite in Constructed Wetlands Z CDs-BOC Nanophotocatalyst Activating Persulfate Under Visible Light for the Efficient Degradation of Typical PPCPs Preparation of pg-C <sub>3</sub> N <sub>4</sub> /BiOBr/Ag Composite and Photocatalytic Degradation of Sulfamethoxazole Sodium Alginate Loading of Zero-Valent Iron Sulfide for the Reduction of Cr( VI) in Water Adsorption Mechanism of Cadmium by Superparamagnetic Nano-Fe <sub>3</sub> O <sub>4</sub> @SiO <sub>2</sub> Functionalized Materials Pollution Characteristics and Removal of Typical Pharmaceuticals in Hospital Wastewater and Municipal Wastewater Treatment Plants Abundance Change of Antibiotic Resistance Genes During PDWW Recycling and Correlations with Environmental Factors Simultaneous Domestication of Short-cut Nitrification Denitrifying Phosphorus Removal Granules Long-term Storage and Rapid Activity Recovery of ANAMMOX Granular Sludge Migration and Environmental Effects of Heavy Metals in the Pyrolysis of Municipal Sludge J Profiling of Antibiotic Resistance Genes in Different Croplands Distribution Characteristics of Antibiotics and Antibiotic Resistance Genes and Microbial Communities in Anaerobic Digestion of Temperature and Stirring on the Changes of Antibiotic Resistance Genes and Microbial Communities in Anaerobic Digestion of Temperature and Stirring on the Changes of Antibiotic Resistance Genes	ments
Hydrochemistry and Its Controlling Factors and Water Quality Assessment of Shallow Groundwater in the Weihe and Jinghe River Cated Characteristics and Drivers of Dissolved Carbon Dioxide and Methane Concentrations in the Nantiaoxi River System in the Upper Reach	ments
Hydrochemistry and Its Controlling Factors and Water Quality Assessment of Shallow Groundwater in the Weihe and Jinghe River Cated Characteristics and Drivers of Dissolved Carbon Dioxide and Methane Concentrations in the Nantiaoxi River System in the Upper Reach Nitrogen Distribution and Inorganic Nitrogen Diffusion Flux in a Shallow Lake During the Low Temperature Period; A Case Study of the Effects of Sediment Microenvironment on Sedimentary Phosphorus Release Under Capping Coadsorption of Heavy Metal and Antibiotic onto Humic Acid from Polder River Sediment Effects of Two PPCPs on Nitrification in Sediments in the Yarlung Zangbo River Wastewater Treatment Effects of Ferric-carbon Micro-electrolysis and Zeolite in Constructed Wetlands Z CDs-BOC Nanophotocatalyst Activating Persulfate Under Visible Light for the Efficient Degradation of Typical PPCPs Preparation of pg-C <sub>3</sub> N <sub>4</sub> /BiOBr/Ag Composite and Photocatalytic Degradation of Sulfamethoxazole Sodium Alginate Loading of Zero-Valent Iron Sulfide for the Reduction of Cr( VI) in Water Adsorption Mechanism of Cadmium by Superparamagnetic Nano-Fe <sub>3</sub> O <sub>4</sub> @SiO <sub>2</sub> Functionalized Materials Pollution Characteristics and Removal of Typical Pharmaceuticals in Hospital Wastewater and Municipal Wastewater Treatment Plants Abundance Change of Antibiotic Resistance Genes During PDWW Recycling and Correlations with Environmental Factors Simultaneous Domestication of Short-cut Nitrification Denitrifying Phosphorus Removal Granules  Long-term Storage and Rapid Activity Recovery of ANAMMOX Granular Sludge Migration and Environmental Effects of Heavy Metals in the Pyrolysis of Municipal Sludge J Profiling of Antibiotic Resistance Genes in Different Croplands  Distribution Characteristics of Antibiotics and Antibiotic Resistance Genes in Manure and Surrounding Soil of Cattle Farms in Ningxia Effects of Temperature and Stirring on the Changes of Antibiotic Resistance Genes and Microbial Communities in Anaerobic Digestion of Temperature and Phosphorus in Soil and Their Influencing F	ments
Hydrochemistry and Its Controlling Factors and Water Quality Assessment of Shallow Groundwater in the Weihe and Jinghe River Cated Characteristics and Drivers of Dissolved Carbon Dioxide and Methane Concentrations in the Nantiaoxi River System in the Upper Reach Nitrogen Distribution and Inorganic Nitrogen Diffusion Flux in a Shallow Lake During the Low Temperature Period; A Case Study of the Effects of Sediment Microenvironment on Sedimentary Phosphorus Release Under Capping Coadsorption of Heavy Metal and Antibiotic onto Humic Acid from Polder River Sediment Effects of Two PPCPs on Nitrification in Sediments in the Yarlung Zangbo River Sediment Effects of Ferric-carbon Micro-electrolysis and Zeolite in Constructed Wetlands Z CDs-BOC Nanophotocatalyst Activating Persulfate Under Visible Light for the Efficient Degradation of Typical PPCPs Sodium Alginate Loading of Zero-Valent Iron Sulfide for the Reduction of Sulfamethoxazole Sodium Alginate Loading of Zero-Valent Iron Sulfide for the Reduction of Cr( VI) in Water Adsorption Mechanism of Cadmium by Superparamagnetic Nano-Fe <sub>2</sub> O <sub>4</sub> @SiO <sub>2</sub> Functionalized Materials Pollution Characteristics and Removal of Typical Pharmaceuticals in Hospital Wastewater and Municipal Wastewater Treatment Plants Abundance Change of Antibiotic Resistance Genes During PDWW Recycling and Correlations with Environmental Factors Simultaneous Domestication of Short-cut Nitrification Denitrifying Phosphorus Removal Granules Ungerem Storage and Rapid Activity Recovery of ANAMMOX Granular Sludge Migration and Environmental Effects of Heavy Metals in the Pyrolysis of Municipal Sludge Migration and Environmental Effects of Heavy Metals in the Pyrolysis of Municipal Sludge Migration of Characteristics of Antibiotics and Antibiotic Resistance Genes in Manure and Surrounding Soil of Cattle Farms in Ningxia Effects of Wheat Straw-derived Biochar Application on Soil Carbon Content Under Different Tillage Practices Spatial Patterns of Nitrogen and Phosphorus in Soil and Their Influencing Factors in	ments
Hydrochemistry and Its Controlling Factors and Water Quality Assessment of Shallow Groundwater in the Weihe and Jinghe River Cated Characteristics and Drivers of Dissolved Carbon Dioxide and Methane Concentrations in the Nantiaoxi River System in the Upper Reach Nitrogen Distribution and Inorganic Nitrogen Diffusion Flux in a Shallow Lake During the Low Temperature Period; A Case Study of the Effects of Sediment Microenvironment on Sedimentary Phosphorus Release Under Capping Coadsorption of Heavy Metal and Antibiotic onto Humic Acid from Polder River Sediment Effects of Two PPCPs on Nitrification in Sediments in the Yarlung Zangbo River Wastewater Treatment Effects of Ferric-carbon Micro-electrolysis and Zeolite in Constructed Wetlands Z CDs-BOC Nanophotocatalyst Activating Persulfate Under Visible Light for the Efficient Degradation of Typical PPCPs Preparation of pg-C <sub>3</sub> N <sub>4</sub> /BiOBt/Ag Composite and Photocatalytic Degradation of Sulfamethoxazole Sodium Alginate Loading of Zero-Valent Iron Sulfide for the Reduction of Cr (VI) in Water Adsorption Mechanism of Cadmium by Superparamagnetic Nano-Fe <sub>3</sub> O <sub>4</sub> @SiO <sub>2</sub> Functionalized Materials Pollution Characteristics and Removal of Typical Pharmaceuticals in Hospital Wastewater and Municipal Wastewater Treatment Plants Abundance Change of Antibiotic Resistance Genes During PDWW Recycling and Correlations with Environmental Factors Simultaneous Domestication of Short-cut Nitrification Denitrifying Phosphorus Removal Granules Long-term Storage and Rapid Activity Recovery of ANAMMOX Granular Sludge Migration and Environmental Effects of Heavy Metals in the Pyrolysis of Municipal Sludge J Profiling of Antibiotic Resistance Genes in Different Croplands Distribution Characteristics of Antibiotics and Antibiotic Resistance Genes in Manure and Surrounding Soil of Cattle Farms in Ningxia Effects of Wheat Straw-derived Biochar Application on Soil Carbon Content Under Different Tillage Practices Spatial Patterns of Nitrogen and Phosphorus in Soil and Their Influencing Factors in a	ments
Hydrochemistry and Its Controlling Factors and Water Quality Assessment of Shallow Groundwater in the Weihe and Jinghe River Cated Characteristics and Drivers of Dissolved Carbon Dioxide and Methane Concentrations in the Nantiaoxi River System in the Upper Reach Nitrogen Distribution and Inorganic Nitrogen Diffusion Flux in a Shallow Lake During the Low Temperature Period; A Case Study of the Effects of Sediment Microenvironment on Sedimentary Phosphorus Release Under Capping Coadsorption of Heavy Metal and Antibiotic onto Humic Acid from Polder River Sediment Effects of Two PPCPs on Nitrification in Sediments in the Yarlung Zangbo River Wastewater Treatment Effects of Ferric-carbon Micro-electrolysis and Zeolite in Constructed Wetlands Z CDs-BOC Nanophotocatalyst Activating Persulfate Under Visible Light for the Efficient Degradation of Typical PPCPs Preparation of pg-C <sub>3</sub> N <sub>4</sub> /BiOBz/Ag Composite and Photocatalytic Degradation of Sulfamethoxazole Sodium Alginate Loading of Zero-Valent Iron Sulfide for the Reduction of Cr( VI) in Water Adsorption Mechanism of Cadmium by Superparamagnetic Nano-Fe <sub>2</sub> O <sub>4</sub> @SiO <sub>2</sub> Functionalized Materials Pollution Characteristics and Removal of Typical Pharmaceuticals in Hospital Wastewater and Municipal Wastewater Treatment Plants Abundance Change of Antibiotic Resistance Genes During PDWW Recycling and Correlations with Environmental Factors Simultaneous Domestication of Short-cut Nitrification Denitrifying Phosphorus Removal Granules Long-term Storage and Rapid Activity Recovery of ANAMMOX Granular Sludge Migration and Environmental Effects of Heavy Metals in the Pyrolysis of Municipal Sludge Distribution Characteristics of Antibiotics and Antibiotic Resistance Genes in Manure and Surrounding Soil of Cattle Farms in Ningxia Effects of Temperature and Stirring on the Changes of Antibiotic Resistance Genes and Microbial Communities in Anaerobic Digestion of Temperature and Stirring on the Changes of Antibiotic Resistance Genes and Microbial Communities in Anaerobic Digestion of Tem	ments
Hydrochemistry and Its Controlling Factors and Water Quality Assessment of Shallow Groundwater in the Weihe and Jinghe River Cated Characteristics and Drivers of Dissolved Carbon Dioxide and Methane Concentrations in the Nantiaoxi River System in the Upper Reach.  Nitrogen Distribution and Inorganic Nitrogen Diffusion Flux in a Shallow Lake During the Low Temperature Period; A Case Study of the Effects of Sediment Microenvironment on Sedimentary Phosphorus Release Under Capping  Coadsorption of Heavy Metal and Antibiotic onto Humie Acid from Polder River Sediment  Effects of Two PPCPs on Nitrification in Sediments in the Yarlung Zangbo River  Wastewater Treatment Effects of Ferric-carbon Micro-electrolysis and Zeolite in Constructed Wetlands  Z CDs-BOC Nanophotocatalyst Activating Persulfate Under Visible Light for the Efficient Degradation of Typical PPCPs  Preparation of pg-C <sub>3</sub> N <sub>4</sub> /BiOBz/Ag Composite and Photocatalytic Degradation of Sulfamethoxazole  Sodium Alginate Loading of Zero-Valent Iron Sulfide for the Reduction of Cr (VI) in Water  Adsorption Mechanism of Cadmium by Superparamagnetic Nano-Fe <sub>3</sub> O <sub>4</sub> @SiO <sub>2</sub> Functionalized Materials  Pollution Characteristics and Removal of Typical Pharmaceuticals in Hospital Wastewater and Municipal Wastewater Treatment Plants:  Abundance Change of Antibiotic Resistance Genes During PDWW Recycling and Correlations with Environmental Factors  Simultaneous Domestication of Short-cut Nitrification Denitrifying Phosphorus Removal Granules  Long-term Storage and Rapid Activity Recovery of ANAMMOX Granular Sludge  Migration and Environmental Effects of Heavy Metals in the Pyrolysis of Municipal Sludge  Migration and Environmental Effects of Heavy Metals in the Pyrolysis of Municipal Sludge  Jerolling of Antibiotic Resistance Genes in Different Croplands  Distribution Characteristics of Antibiotics and Antibiotic Resistance Genes and Microbial Communities in Anaerobic Digestion of Cappalar Patterns of Nitrogen and Phosphorus in Soil and Their Influencing Factors in a Typical	ments
Hydrochemistry and Its Controlling Factors and Water Quality Assessment of Shallow Groundwater in the Weihe and Jinghe River Catel Characteristics and Drivers of Dissolved Carbon Dioxide and Methane Concentrations in the Nantiaoxi River System in the Upper Reach Nitrogen Distribution and Inorganic Nitrogen Diffusion Flux in a Shallow Lake During the Low Temperature Period; A Case Study of the Effects of Sediment Microenvironment on Sedimentary Phosphorus Release Under Capping Coadsorption of Heavy Metal and Antibiotic onto Humic Acid from Polder River Sediment Effects of Two PPCPs on Nitrification in Sediments in the Yarlung Zangbo River  Wastewater Treatment Effects of Ferric-carbon Micro-electrolysis and Zeolite in Constructed Wetlands ZCOb-BOC Nanophotocatalyst Activating Persulfate Under Visible Light for the Efficient Degradation of Typical PPCPs Preparation of pg-C <sub>3</sub> N <sub>4</sub> /BiOBr/Ag Composite and Photocatalytic Degradation of Sulfamethoxazole Sodium Alginate Loading of Zero-Valent Iron Sulfide for the Reduction of Cr(VI) in Water Adsorption Mechanism of Cadmium by Superparamagnetic Nano-Fe <sub>3</sub> O <sub>4</sub> @SiO <sub>2</sub> Functionalized Materials Pollution Characteristics and Removal of Typical Pharmaceuticals in Hospital Wastewater and Municipal Wastewater Treatment Plants - Abundance Change of Antibiotic Resistance Genes During PDWW Recycling and Correlations with Environmental Factors Simultaneous Domestication of Short-cut Nitrification Denitrifying Phosphorus Removal Granules   Long-term Storage and Rapid Activity Recovery of ANAMMOX Granular Sludge   Migration and Environmental Effects of Heavy Metals in the Pyrolysis of Municipal Sludge   Jo Profiling of Antibiotic Resistance Genes in Different Croplands   Distribution Characteristics of Antibiotics and Antibiotic Resistance Genes and Microbial Communities in Anaerobic Digestion of Temperature and Stirring on the Changes of Antibiotic Resistance Genes and Microbial Communities in Anaerobic Digestion of Temperature and Stirring on the Changes of Antibiotic Resistance Ge	ments
Hydrochemistry and Its Controlling Factors and Water Quality Assessment of Shallow Groundwater in the Weihe and Jinghe River Cated Characteristics and Drivers of Dissolved Carbon Dioxide and Methane Concentrations in the Nantiaoxi River System in the Upper Reach Nitrogen Distribution and Inorganic Nitrogen Diffusion Flux in a Shallow Lake During the Low Temperature Period: A Case Study of the Effects of Sediment Microenvironment on Sedimentary Phosphorus Release Under Capping Coadsorption of Heavy Metal and Antibiotic onto Humic Acid from Polder River Sediment Effects of Two PPCPs on Nitrification in Sediments in the Yarlung Zangbo River Wastewater Treatment Effects of Ferric-carbon Micro-electrolysis and Zeolite in Constructed Wetlands Z COb-BOC Nanophotocatalyst Activating Persulfate Under Visible Light for the Efficient Degradation of Typical PPCPs Preparation of pg-C <sub>3</sub> N <sub>4</sub> /BiOBr/Ag Composite and Photocatalytic Degradation of Sulfamethoxazole Sodium Alginate Loading of Zero-Valent Iron Sulfide for the Reduction of Cr( VI) in Water Adsorption Mechanism of Cadmium by Superparamagnetic Nano-Fe <sub>3</sub> O <sub>4</sub> @SiO <sub>2</sub> Functionalized Materials Pollution Characteristics and Removal of Typical Pharmaceuticals in Hospital Wastewater and Municipal Wastewater Treatment Plants Abundance Change of Antibiotic Resistance Genes During PDWW Recycling and Correlations with Environmental Factors Simultaneous Domestication of Short-cut Nitrification Denitrifying Phosphorus Removal Granules Long-term Storage and Rapid Activity Recovery of ANAMMOX Granular Sludge Migration and Environmental Effects of Heavy Metals in the Pyrolysis of Municipal Sludge Migration and Environmental Effects of Heavy Metals in the Pyrolysis of Municipal Sludge Profiling of Antibiotic Resistance Genes in Different Croplands  Effects of Temperature and Stirring on the Changes of Antibiotic Resistance Genes and Microbial Communities in Anaerobic Digestion of Temperature and Stirring on the Changes of Antibiotic Resistance Genes and Microbial Communities in Anaero	ments LIU Xin, XIANG Wei, SI Bing-cheng (2817) es of the Taihu Lake Basin During Summer-Autumn  LIANG Jia-hui, TIAN Lin-lin, ZHOU Zhong-yu, et al. (2826) e Baiyangdian Lake
Hydrochemistry and Its Controlling Factors and Water Quality Assessment of Shallow Groundwater in the Weihe and Jinghe River Catel Characteristics and Drivers of Dissolved Carbon Dioxide and Methane Concentrations in the Nantiaoxi River System in the Upper Reach Nitrogen Distribution and Inorganic Nitrogen Diffusion Flux in a Shallow Lake During the Low Temperature Period; A Case Study of the Effects of Sediment Microenvironment on Sedimentary Phosphorus Release Under Capping Coadsorption of Heavy Metal and Antibiotic onto Humic Acid from Polder River Sediment Effects of Two PPCPs on Nitrification in Sediments in the Yarlung Zangbo River  Wastewater Treatment Effects of Ferric-carbon Micro-electrolysis and Zeolite in Constructed Wetlands ZCOb-BOC Nanophotocatalyst Activating Persulfate Under Visible Light for the Efficient Degradation of Typical PPCPs Preparation of pg-C <sub>3</sub> N <sub>4</sub> /BiOBr/Ag Composite and Photocatalytic Degradation of Sulfamethoxazole Sodium Alginate Loading of Zero-Valent Iron Sulfide for the Reduction of Cr(VI) in Water Adsorption Mechanism of Cadmium by Superparamagnetic Nano-Fe <sub>3</sub> O <sub>4</sub> @SiO <sub>2</sub> Functionalized Materials Pollution Characteristics and Removal of Typical Pharmaceuticals in Hospital Wastewater and Municipal Wastewater Treatment Plants - Abundance Change of Antibiotic Resistance Genes During PDWW Recycling and Correlations with Environmental Factors Simultaneous Domestication of Short-cut Nitrification Denitrifying Phosphorus Removal Granules   Long-term Storage and Rapid Activity Recovery of ANAMMOX Granular Sludge   Migration and Environmental Effects of Heavy Metals in the Pyrolysis of Municipal Sludge   Jo Profiling of Antibiotic Resistance Genes in Different Croplands   Distribution Characteristics of Antibiotics and Antibiotic Resistance Genes and Microbial Communities in Anaerobic Digestion of Temperature and Stirring on the Changes of Antibiotic Resistance Genes and Microbial Communities in Anaerobic Digestion of Temperature and Stirring on the Changes of Antibiotic Resistance Ge	ments